A Distributed Antenna Tuning Unit Using a Frequency Reconfigurable PIXEL-Antenna

Alfred Grau*, and Franco De Flaviis†

*Broadcom Corporation, 5300 California Ave., Irvine, CA 92617, USA; agrau@broadcom.com

† University of California at Irvine, 2233 Engineering Gateway, UCI, 92697-7625 Irvine, CA, USA; franco@uci.edu

***Abstract*—In this work we present the design and performance analysis of a distributed antenna tuning unit using a frequency reconfigurable PIXEL antenna. The proposed tuning unit is distributed in the sense that it brings together the antenna and the traditional reconfigurable matching network (typically implemented with inductors and switched capacitors) into a reconfigurable antenna. As a result, the losses introduced by a reconfigurable matching network are eliminated, although additional complexity is put into the antenna system. Also, the proposed distributed system can use additional degrees of freedom provided by the PIXEL antenna (e.g. tunable radiation pattern) to minimize the interactions with the human body and thus help on the tuning of the antenna impedance. Results on the impedance tuning capabilities are presented.**

I. Introduction

Years of theoretical studies and experimentation have shown that the impedance of any antenna is determined by its shape, size and material composition. However, the impedance of an antenna, specially when located within a particular communication device, will also depend on the surrounding components to the antenna (specially if those are metallic), and on the interactions with the user's body (such as the hand and the head). Having the capability to dynamically adapt the impedance of an antenna and transform it into a desired one is becoming a very desirable feature in wireless communication systems. Systems that implement this capability are known as antenna tuning units [7], [4]. Therefore, these units usually can transform a finite set of arbitrary antenna impedance into a desirable one (normally 50Ω). As a result, these units allows one to recover the mismatch between the antenna and the subsequent modules (e.g. antenna switch). In addition, because a desirable impedance is presented at the beginning of the radio-frequency chain, other elements of such chain, such as the power amplifiers and low noise amplifiers, are able to work closer to its optimal conditions, thus boosting the performance of the wireless communicating device.

Typically, these antenna tuning units are composed of a reconfigurable matching network (implemented using inductor and switched capacitors), a coupler (to determine the reflection coefficient of the antenna after the reconfigurable matching network), and a control unit, which is responsible for selecting the best state of the reconfigurable matching network (i.e. the one that minimizes the return loss) and for continuously updating the system.

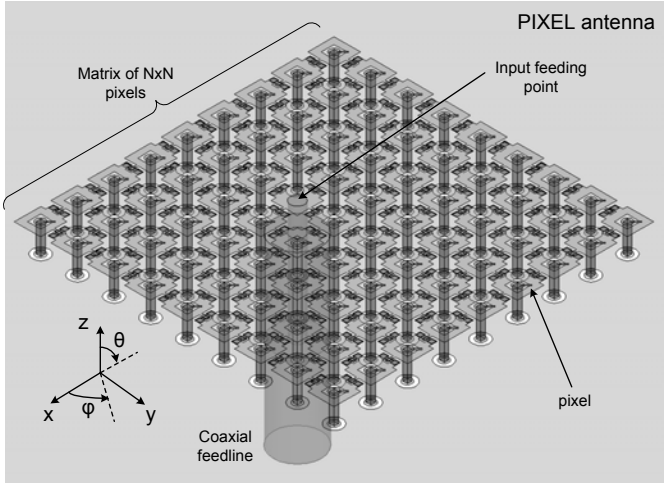

Figure 1. Geometry model and dimensions of a generic $N \times N$ PIXEL antenna.

In this paper we propose an alternative implementation for an antenna tuning unit which eliminates the need of the reconfigurable matching network. The proposed system consist of a distributed antenna tuning unit using a frequency reconfigurable PIXEL antenna. That it, the proposed tuning unit is distributed in the sense that it brings together the antenna and the traditional reconfigurable matching network (typically implemented with inductors and switched capacitors) into a reconfigurable antenna which we describe in the next section. This distributed implementation of an antenna tuning unit has the advantage of attacking the mismatch problem at the antenna level. Therefore, the losses introduced by a matching network are eliminated, although additional complexity is put into the antenna system. It can also be shown that the proposed distributed system can use additional degrees of freedom provided by the PIXEL antenna (e.g. tunable radiation pattern) to minimize the interactions with the human body and thus help on the tuning of the antenna impedance.

II. PIXEL Antenna

The PIXEL antenna [2][5][6] can be described as a microstrip radiator composed of an $N \times N$ matrix of metallic pixels interconnected through MEMS switches. Each one

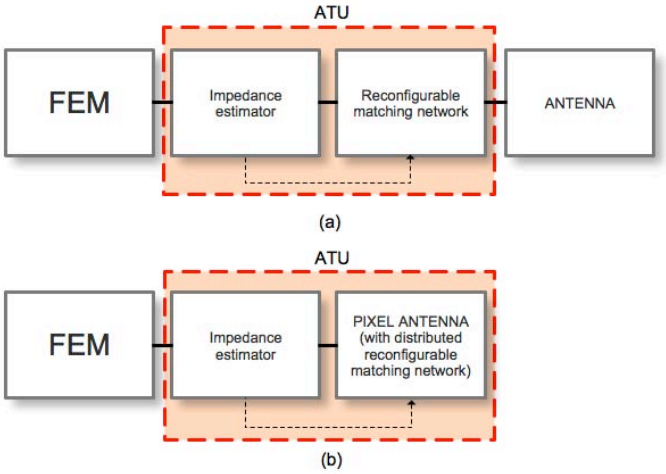

Figure 2. Simplified block diagram of a communication system's radio-frequency chain employing an antenna tuning unit, (a) in a traditional approach, and (b) for the proposed antenna tuning unit paradigm using the PIXEL antenna.

of the N^2 metallic pixels has a square shape, with some intrusions to allocate the MEMS switches and the biasing system. The basic principle of operation of the PIXEL antenna is as follows: by interconnecting specific sets of pixels within this matrix, several radiating structures can be mapped, such as circular, rectangular, triangular, and comb patches [2], among others. These distinct mapped patches ultimately radiate through distinct operating frequencies. Fig. 1 shows the geometry model of a generic $N \times N$ PIXEL antenna.

As shown in Fig. 1, the antenna is fed through a coaxial cable. The inner conductor of the coaxial connects to one of the metallic pixels of the radiator, while the external conductor connects to the ground plane. Notice that the feed point is always at a fix location. That is, the pixel connected to the inner connector of the coaxial is always the same in all possible configurations of the PIXEL antenna. Therefore, due to the fact that a good impedance match is normally achieved at a certain offset from the center of a microstrip patch [1], [8], the microstrip patches must be mapped with the necessary offset with respect to the feeding pixel in order to preserve a good impedance match (i.e. such that the input impedance that they present is as close to 50Ω as possible).

In our design, the number of pixels per dimension is $N = 9$, each metallic pixel has dimensions $1.43 \times 1.43mm^2$, and they are separated $2mm$ from each other. Qualitatively speaking, the pixels dimensions were chosen to maximize the number of functionalities that the antenna can generate (i.e. the smaller possible pixel dimension), for a given pixeled area, while ensuring enough space to allocate the MEMS switches and biasing system (i.e. vias, nichrome lines, etc.). The PIXEL antenna has been simulated using a substrate of dimensions $50.8 \times 50.8mm^2$, with a thickness of $1.5875mm$. The dielectric constant and loss tangent of the PCB substrate (RO-TMM3) is $\epsilon_r = 3.78$ and $\tan\delta = 0.002$.

III. Distributed Antenna Tuning Unit

When using the PIXEL antenna within the proposed distributed antenna tuning unit system, once a particular patch has been mapped into the matrix of metallic pixels, it is possible to adjust the input impedance value that it presents at the feed point by connecting or disconnecting strategically chosen pixels from within the interconnected parts of the aperture, or from the surrounding region using the pixels as parasitic elements. This impedance matching capability constitutes a very important functionality (to be used in the proposed distributed antenna tuning unit), which can be combined, as well, with the capability to reconfigure the resonant frequency of the antenna. The reason has to do with the fact that this capability can then be used to compensate for undesired changes in impedance as a result of the interaction of the antenna with the human body of the user or with the surrounding components. Notice that this impedance matching is not being conducted at the feedline level (as it is traditionally done using reconfigurable matching networks of inductors and switched capacitors), but instead on a distributed manner within the radiating structure itself.

On the other hand, for a particular resonant frequency, the PIXEL antenna is capable of exciting multiple radiation modes (such as the transverse magnetic modes TM1, TM2 and TM0 modes of a circular patch, as defined in [8]). This capability can also be used by the proposed tuning unit. In fact, in a first step, the proposed system can select, among this set of radiation patterns, the one that minimizes the interaction with the human body, and later on, in a second step, refine the set of connected and disconnected pixels to further adjust the input impedance of the antenna (through monitoring the reflection coefficient) to be as close as possible to the desired 50Ω one. In this work, however, we focus on the impedance matching capability and we leave the study of the advantages of pattern reconfigurability as future work.

Fig. 2 shows a simplified block diagram of a communication system's radio-frequency (RF) chain employing an antenna tuning unit, (a) in a traditional approach, and (b) for the proposed distributed antenna tuning unit paradigm using the PIXEL antenna. In the block diagram, FEM stands for Front End Module (which includes the power amplifier, duplexers, filters, and other RF components), while the impedance estimator typically includes a bidirectional coupler and power detectors which are used to estimate the magnitude and/or phase of the reflection coefficient (Γ_{IN}) looking towards the reconfigurable matching network (and antenna). In both approaches, the antenna tuning unit works as follow: at the beginning of a specific data frame the system will estimate the impedance of the antenna; if it found that the impedance is not 50Ω it will adapt either the reconfigurable matching network or the PIXEL antenna to transform its impedance into 50Ω. The optimal solution can be found by performing a full search of the solution space or by using some searching algorithm. In this work, we use a generic genetic algorithm.

To demonstrate the effectiveness of the PIXEL antenna as a distributed impedance matching network, we have considered

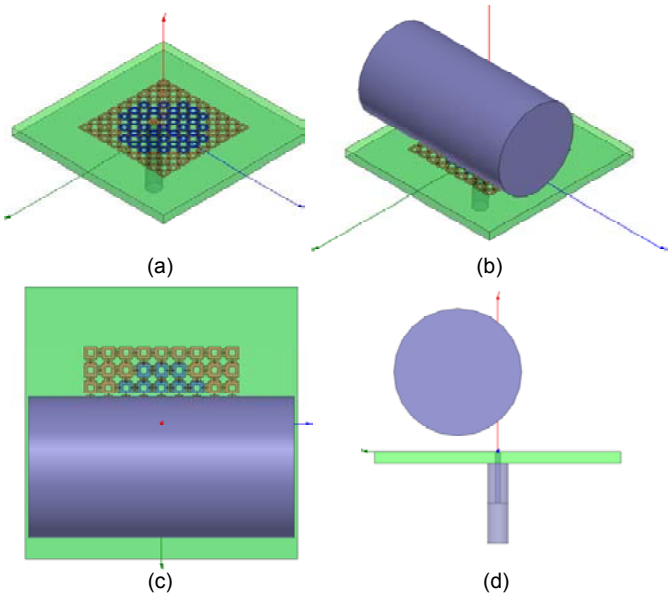

Figure 3. Several views of the PIXEL antenna: (a) perspective view of the standalone PIXEL antenna, and (b) (c) (d) show the perspective, top and side view, respectively of the PIXEL antenna in close proximity of a perfect electric conductor (PEC) cylinder.

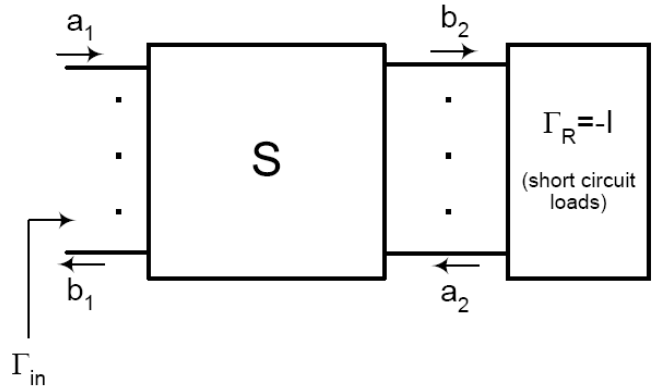

Figure 4. Network model representation of the PIXEL antenna. In the figure, a_1 and b_1 represent the input and reflected waves in the feeding coaxial cable of the antenna. The waves at interface 2 (a_2 and b_2) represent the incident and reflected waves on each one of the Q MEMS switches distributed across the pixeled aperture of the PIXEL antenna. Notice that if the reflection coefficient at the i^{th} port is set to be $\Gamma_{R_{ii}} = -1$ then the i^{th} MEMS switch will be in an ON state. On the other hand, if the reflection coefficient at the i^{th} port is set to be $\Gamma_{R_{ii}} = 1$ then the i^{th} MEMS switch will be in an OFF state.

two scenarios. In the first scenario, the PIXEL antenna is placed standalone on air and the MEMS switches are configured to make the antenna resonate at $5.5GHz$ using the TM1 mode. In a second scenario, a perfect electric conductor (PEC) cylinder of $8mm$ radius and $13mm$ length is brought close to the PIXEL antenna. The closest edge of the cylinder is at a distance of $7mm$ from the metallic aperture, and slightly off the center of the PIXEL antenna by $5mm$. As it will be shown, the PEC cylinder perturbs the near field of the antenna and thus the PIXEL antenna becomes mismatch at $5.5GHz$. Then, we connect a genetic algorithm to the PIXEL antenna and we let it readapt itself to bring a resonance at the desired frequency. Fig. 3 shows several views of two scenarios commented above.

In order to efficiently connect a genetic algorithm to the PIXEL, we first performed a full-wave simulation of the problem's geometry using the finite element method electromagnetic solver from Ansoft Corporation, HFSS [3], for each one of the two abovementioned scenarios (for the standalone PIXEL antenna (Fig. 3 (a)), and for the PIXEL antenna with the PEC cylinder (Fig. 3 (b))). In these simulations, each one of the 144 MEMS switches of the PIXEL antenna have been replaced with a lumped port. In this manner, only a single full-wave simulation is required to evaluate the response of the antenna for its 2^{144} possible configurations. Notice that the number of configurations results from the fact that each MEMS switch can either be in an ON or OFF state. From the simulation data, the scattering parameter matrix S is exported. This matrix has dimensions 145×145 because the total number of ports of the problem is 145 ($Q = 144$ ports corresponding to the MEMS switches and $P = 1$ additional port corresponding to the coaxial feed of the antenna), and thus can be expressed in the form:

$$S = \begin{pmatrix} S_{11}^{PxP} & S_{12}^{PxQ} \\ S_{21}^{QxP} & S_{22}^{QxQ} \end{pmatrix} \quad (1)$$

It can then be shown that the reflection coefficient at the coaxial input port of the PIXEL antenna is given by:

$$\Gamma_{IN} = S_{11}^{PxP} + S_{12}^{PxQ}\left(I^{QxQ} - \Gamma_R S_{22}^{QxQ}\right)^{-1}\Gamma_R S_{21}^{QxP} \quad (2)$$

where Γ_R is a diagonal matrix of the form:

$$\Gamma_R = \begin{pmatrix} \Gamma_{R_{11}} & 0 & \cdots & 0 & 0 \\ 0 & \Gamma_{R_{22}} & 0 & 0 & 0 \\ \vdots & 0 & \ddots & 0 & \vdots \\ 0 & 0 & 0 & \ddots & \\ 0 & 0 & \cdots & 0 & \Gamma_{R_{QQ}} \end{pmatrix} \quad (3)$$

where the variables $\Gamma_{R_{ii}}$ can either take the value 1 or -1. The abovementioned simulation procedure and a network model representation of the PIXEL antenna is illustrated in Fig. 4. In this figure, a_1 and b_1 represent the input and reflected waves in the feeding coaxial cable of the antenna. The waves at interface 2 (a_2 and b_2) represent the incident and reflected waves on each one of the Q MEMS switches distributed across the pixeled aperture of the PIXEL antenna. Notice that if the reflection coefficient at the i^{th} port is set to be $\Gamma_{R_{ii}} = -1$ then the i^{th} MEMS switch will be in an ON state. On the other hand, if the reflection coefficient at the i^{th} port is set to be $\Gamma_{R_{ii}} = 1$ then the i^{th} MEMS switch will be in an OFF state.

At this point, we feed this information into a genetic algorithm that evaluates a specific fitness function to arrive at the optimal solution. In particular, the algorithm will stop its search after the minimization of the fitness function (FF)

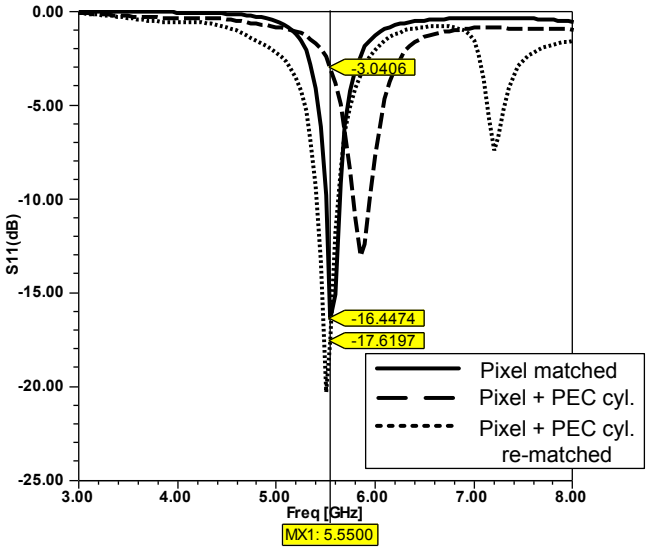

Figure 5. Return loss response of the PIXEL antenna in several scenarios: matched case for the standalone PIXEL (solid line), mismatched as a result of the PEC cylinder (dashed line), and re-matched after adjusting the interconnected pixels of the antenna to compensate the mismatch effects of the PEC cylinder (dotted line).

$FF = 20\log_{10}(|\Gamma_{IN}|)$. The optimal reflection coefficient is then given by:

$$\Gamma_{R_{opt}} = \min_{\Gamma_R}(20\log_{10}(|\Gamma_{IN}|)) \quad (4)$$

Notice that the abovementioned FF can be evaluated at a single frequency or over frequency range. In our case, the optimizations were conducted at a single frequency of $5.5GHz$. Also, notice that once an optimal solution ($\Gamma_{R_{opt}}$) has been obtained, the state of the MEMS switches of the PIXEL antenna is readily found by a simple inspection of the diagonal elements in the matrix, as described above.

IV. SIMULATION RESULTS

As we will shown in this section, the PIXEL antenna has the capability to transform its input impedance to a value close to 50Ω, in the two abovementioned scenarios. Fig. 5 shows the return loss response of the PIXEL antenna in several scenarios: matched case for the standalone PIXEL (solid line), mismatched as a result of the PEC cylinder (dashed line), and re-matched after adjusting the interconnected pixels of the antenna to compensate the mismatch effects of the PEC cylinder (dotted line). We observe that the initial matching level at $5.5GHz$ is around $-16.4dB$ (this solution was obtained after running a full wave simulation of the standalone PIXEL antenna on air and letting the genetic optimizer minimize the reflection coefficient at the frequency of interest). However, when the PEC cylinder is approached to the antenna, the return loss level degrades to a level around $-3dB$. Then, we let the PIXEL antenna readjust the states of the MEMS switches within the pixel aperture in order to recover the matching level. The optimal solution was able to successfully rematch the

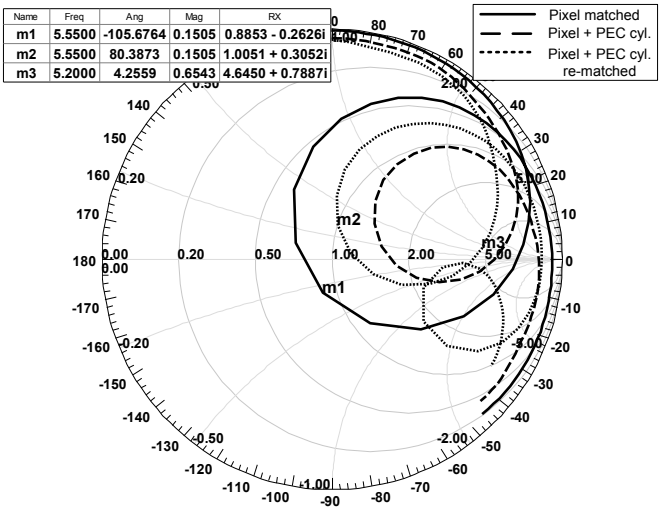

Figure 6. Representation of the antenna input impedance in several scenarios: matched case for the standalone PIXEL (solid line), mismatched as a result of the PEC cylinder (dashed line), and re-matched after adjusting the interconnected pixels of the antenna to compensate the mismatch effects of the PEC cylinder (dotted line).

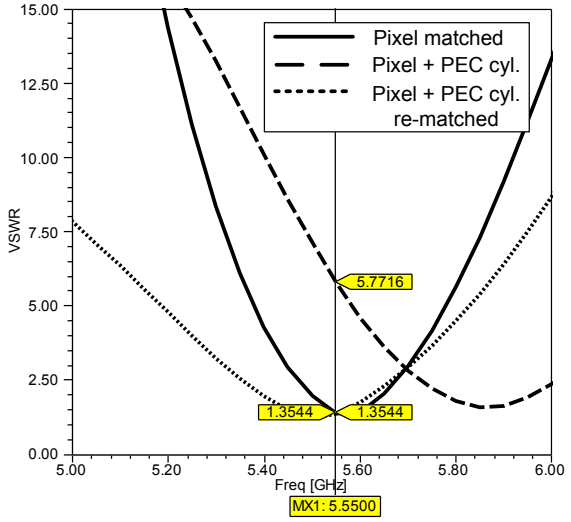

Figure 7. VSWR response of the PIXEL antenna in several scenarios: matched case for the standalone PIXEL (solid line), mismatched as a result of the PEC cylinder (dashed line), and re-matched after adjusting the interconnected pixels of the antenna to compensate the mismatch effects of the PEC cylinder (dotted line).

antenna at a level around $-17.6dB$. Notice that, again, this solution was obtained after running a full wave simulation of the PIXEL antenna in close proximity to the PEC cylinder and letting the genetic optimizer minimize the reflection coefficient at the frequency of interest.

Figs. 6 and 7 illustrate equivalent representations of these results using different figures of merit: the complex input impedance and the voltage standing wave ratio (VSWR), respectively. We observe that the PIXEL antenna is able to recover a mismatched VSWR of around 5.77 by lowering it to near 1.35. Notice that a VSWR of 5 is a very common

situation in cellular and WLAN communication systems, thus proving the interest for the PIXEL antenna as a distributed antenna tuning unit.

In Fig. 8, it is shown the 3D realized gain patterns of the PIXEL antenna in several scenarios: (a) matched case for the standalone PIXEL, (c) mismatched as a result of the PEC cylinder, and (b) re-matched after adjusting the interconnected pixels of the antenna to compensate the mismatch effects of the PEC cylinder. Notice that the realized gain implicitly takes into consideration the mismatch level and radiation efficiency characteristics of the antenna. The maximum realized gain in the original matched case is $6.17dBi$. On the other hand, when the PEC cylinder is brought close to the PIXEL antenna the realized gain drops to $-3.68dBi$ as a result of poor matching and radiation efficiency, and distortion in the radiation pattern. When the PIXEL antenna is rematched, the realized gain improves to $-1.14dBi$ due to better matching, however we observe that the radiation efficiency is still poor and the radiation pattern remains distorted. It is left as future work to investigate if the the radiation efficiency can be improved by means of exciting higher order modes (TM2 or TM0) which may spread the radiated energy towards directions away from the PEC cylinder.

Finally, Fig. 9 shows a representation of the set of interconnected pixels (in blue) for (a) the original matched case, and (b) for the re-matched case after adjusting the interconnected pixels of the antenna to compensate the mismatch effects of the PEC cylinder. Pixels in light red color represent pixels disconnected from the main mapped aperture.

As a final note, notice that additional simulations have been conducted using cylindrical objects of different material (dielectrics) and slightly different sizes and similar response were obtained. However, a more extensive investigation is required to determine the limits of tuning range of the PIXEL antenna as a distributed antenna tuning unit.

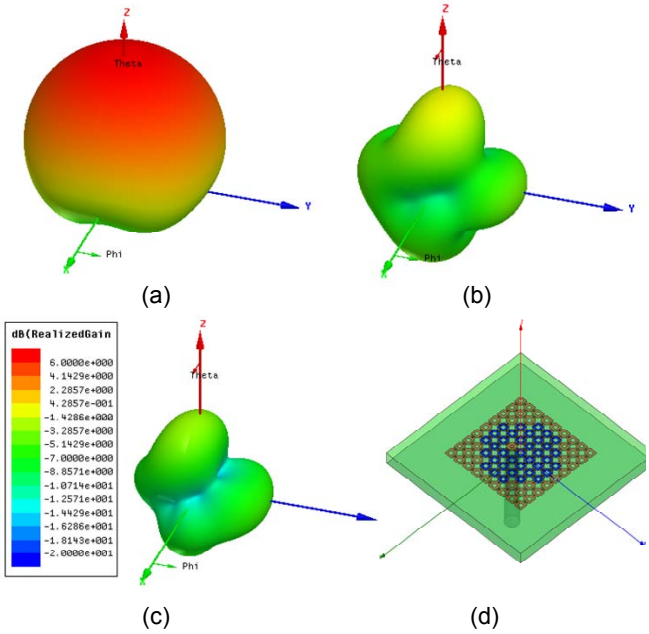

Figure 8. Realized gain patterns of the PIXEL antenna in several scenarios: (a) matched case for the standalone PIXEL, (c) mismatched as a result of the PEC cylinder, and (b) re-matched after adjusting the interconnected pixels of the antenna to compensate the mismatch effects of the PEC cylinder. In (d) it is shown a perspective view of the PIXEL antenna with the used coordinate system referenced on it.

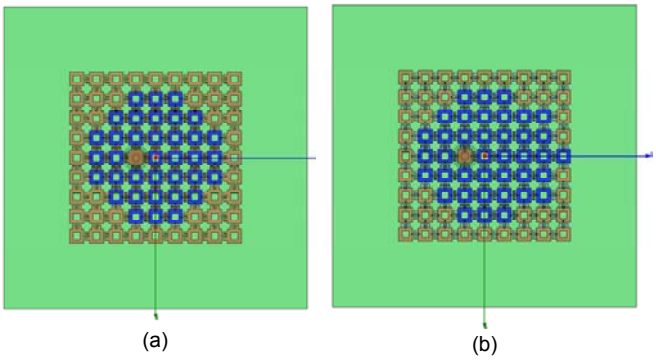

Figure 9. Representation of the set of interconnected pixels (in blue) for (a) the original matched case, and (b) for the re-matched case after adjusting the interconnected pixels of the antenna to compensate the mismatch effects of the PEC cylinder. Pixels in light red color represent pixels disconnected from the main mapped aperture.

V. CONCLUSIONS

The feasibility of a distributed antenna tuning unit using a MEMS frequency reconfigurable PIXEL-antennas has been demonstrated. The proposed tuning unit is distributed in the sense that it brings together the antenna and the traditional reconfigurable matching network (typically implemented with inductors and switched capacitors) into a reconfigurable antenna. Results on the impedance tuning capabilities have been presented.

REFERENCES

[1] Constantine A. Balanis. *Antenna Theory, Analysis and Design*. John Wiley and Sons Inc., 2nd edition, 1997.

[2] B.A. Cetiner, H. Jafarkhani, Jiang-Yuan Qian, Hui Jae Yoo, A. Grau, and F. De Flaviis. Multifunctional reconfigurable MEMS integrated antennas for adaptive MIMO systems. *Communications Magazine, IEEE*, 42(12):62–70, Dec 2004.

[3] Ansoft Corp. http://www.ansoft.com.

[4] J. de Mingo, A. Valdovinos, A. Crespo, D. Navarro, and P. Garcia. An RF electronically controlled impedance tuning network design and its application to an antenna input impedance automatic matching system. *Microwave Theory and Techniques, IEEE Transactions on*, 52(2):489–497, Feb. 2004.

[5] A. Grau, J. Romeu, L. Jofre, and F. De Flaviis. A software defined MEMS-reconfigurable PIXEL-antenna for narrowband MIMO systems. In *Adaptive Hardware and Systems, 2008. AHS '08. NASA/ESA Conference on*, pages 141–146, June 2008.

[6] Alfred Grau and Franco De Flaviis. A software defined antenna using MEMS technology on printed circuit board. *Antennas and Propagation,* IEEE *Transactions on (submitted)*, 2009.

[7] H. Song, S.-H. Oh, J.T. Aberle, B. Bakkaloglu, and C. Chakrabarti. Automatic antenna tuning unit for software-defined and cognitive radio. In *Antennas and Propagation Society International Symposium, 2007 IEEE*, pages 85–88, June 2007.

[8] Rodney G. Vaughan. Two-port higher mode circular microstrip antennas. *Antennas and Propagation, IEEE Transactions on*, 36(3):309–321, Mar 1988.